Atomic structure of the sweet-tasting protein thaumatin I at pH 8.0 reveals the large disulfide-rich region in domain II to be sensitive to a pH change

Tetsuya Masuda[ab]*, Keisuke Ohta[ab], Bunzo Mikami[c] , Naofumi Kitabatake[d] , and Fumito Tani[ab]

[a]Division of Food Science and Biotechnology, Graduate School of Agriculture, Kyoto University, Gokasho, Uji, Kyoto, 611-0011, Japan, [b]Department of Natural Resources, Graduate School of Global Environmental Studies, Kyoto University, Gokasho, Uji, Kyoto, 611-0011, Japan, and [c]Division of Applied Life Sciences, Graduate School of Agriculture, Kyoto University, Gokasho, Uji, Kyoto, 611-0011, Japan and [d]Department of Foods and Human Nutrition, Notre Dame Seishin University, Okayama 700-8516, Japan

Correspondence email: t2masuda@kais.kyoto-u.ac.jp

Abstract

Thaumatin, an intensely sweet-tasting plant protein, elicits a sweet taste at 50 nM. Although the sweetness remains when thaumatin is heated at 80°C for 4 h under acid conditions, it rapidly declines when heating at a pH above 7.0. To clarify the structural difference at high pH, the atomic structure of a recombinant thaumatin I at pH 8.0 was determined at a resolution of 1.0 Å. Comparison to the crystal structure of thaumatin at pH 7.3 and 6.5 revealed the root-mean square deviation value of a Cα atom to be substantially greater in the large disulfide-rich region of domain II, especially residues 154-164, suggesting that a loop region in domain II to be affected by solvent conditions. Furthermore, *B*-factors of Lys137, Lys163 and Lys187 were significantly affected by pH change, suggesting that a striking increase in the mobility of these lysine residues, which could facilitate a reaction with a free sulfhydryl residue produced via the β-elimination of disulfide bonds by heating at a pH above 7.0. The increase in mobility of lysine residues as well as a loop region in domain II might play an important role in the heat-induced aggregation of thaumatin above pH 7.0.

Keywords: thaumatin, sweet-tasting protein, alkaline conditions, heat, shelxl, hydrogen-atoms

1. Introduction

Thaumatin is a sweet-tasting protein that elicits a sweet taste sensation at 50 nM. Since it is nearly 100,000 times sweeter than sucrose on a molar basis [1], thaumatin has potential as a low-calorie sweetener for industrial applications and could be useful for clarifying the mechanisms of perception of sweet taste [2-4]. Thaumatin is isolated from the arils of *Thaumatococcus daniellii* Benth, a plant native to tropical West Africa. At least five intensely sweet forms of protein exist in the plant, with two major components (thaumatin I and thaumatin II) and three minor components (thaumatin a, b, and c) [1]. All of them have been accepted as a food material because they are natural proteins [5]. Since the source of thaumatin contains some variants, mainly thaumatin I and thaumatin II, further purification by cation exchange chromatography tends to be required for an atomic resolution-based structural analysis [6,7]. The three-dimensional structure of thaumatin has been determined and consists of three domains; (1) an 11-stranded core domain (1-53, 85-127 and 178-207, domain I); (2) a large disulfide-rich region (128-177, domain II); and (3) a small disulfide-rich region (54-84, domain III) [6-16]. Recently, a homogeneous recombinant thaumatin I was successfully obtained from the yeast *Pichia pastoris* [17,18] and electron density maps of some residues in this recombinant thaumatin I were significantly improved to clarify subtle structural variations when compared to purified plant thaumatin I [7].

Thaumatin contains no cysteine residues but eight intramolecular disulfide bonds [1,19]. Although the protein does not contain a free cysteine residue, intermolecular disulfide linkages are formed by heating thaumatin at a pH above 7.0, causing its sweetness to disappear [20]. In contrast, its sweetness remains when heated at 80°C for 4 h under acid conditions [21]. The reduction in sweetness caused by heating at above pH 7.0 would be attributed to the formation of aggregates and the disulfide interchange reaction was catalyzed by cysteine; that is, a free sulfhydryl residue was

formed via the β-elimination of a disulfide bond [20]. Thus the thermo inactivation of thaumatin was largely dependent on pH, however, high resolution structural comparisons of thaumatin at different pH have not been performed.

To date, high resolution structures of thaumatin have been reported for crystals of the orthorhombic form and tetragonal form [6,7,11-13]. Comparisons at an atomic resolution have enabled us to clarify subtle structural differences among the thaumatin variants [16] and provided detailed structural information on protein molecules by including the hydrogen atoms [7].

In the present study, the atomic structure of a recombinant thaumatin I at pH 8.0 was determined at a resolution of 1.0 Å. The similarities and differences in the refined structure of the recombinant thaumatin I as well as plant thaumatin I under alkaline conditions were investigated in detail. Comparisons at pH 7.3 revealed the large disulfide-rich region of domain II, especially residues 153-164 to be markedly affected by pH change. Furthermore, *B*-factors of Lys137, Lys163, and Lys187 were substantially increased. Since it was suggested that the heat-inactivation of thaumatin involved lysine residues and a free sulfhydryl residue produced via the β-elimination of disulfide bonds by heating at a pH above 7 [20], increases in the mobility of lysine residues as well as the large disulfide-rich region in domain II under alkaline conditions might play an important role in the heat-induced aggregation of thaumatin above pH 7.0.

2. Materials and methods

2.1. Materials

Plant thaumatin was purchased from Wako Pure Chemical Industries Ltd. and further purified as described [20]. Polyethylene glycol 3350 was obtained from Sigma-Aldrich (St. Louis, MO). The specially prepared reagent of tris(hydroxymethyl)aminomethane was from Nacalai Tesque Inc.

(Kyoto, Japan). All other chemicals were of guaranteed reagent grade for biochemical use.

2.2. Expression and purification of the recombinant thaumatin I

The expression of the recombinant thaumatin I was performed with *P. pastoris* as described previously [18,22]. A 7-L fermenter (TS-M7L, Takasugi Seisakusho Co., Tokyo, Japan) was used for secretion of the recombinant thaumatin I into the medium. Purification was performed with an SP-Sephadex C-25 cation exchange column, and followed by HW-50F gel-filtration chromatography (Tosoh Co., Tokyo, Japan). The concentrations of thaumatin were determined spectrophotometrically using a molar extinction coefficient, ε_{278}, of 17,000 /M cm [1]. The purity of proteins was checked by both SDS-PAGE and native-PAGE.

2.3. Crystallization and data collection

The purified recombinant thaumatin was concentrated by a Centricon 10 (Millipore, Bedford, MA), and the protein concentration was measured with a NanoDrop ND-1000 spectrophotometer (NanoDrop Technologies, Inc., Rockland, DE). Crystallization was performed by using the hanging-drop vapor-diffusion method. The hanging drops were prepared by mixing 5 μL of the 30-50 mg/mL protein solutions and 5 μL of the reservoir solution. The reservoir solution consisted of 50 mM Tris-HCl buffer, pH 8.0 containing 15% PEG3350. All solutions were prepared with sterile water and filtrated with a MILLEXGV membrane (Millipore). Under these conditions, crystals with the orthorhombic form in space group $P2_12_12_1$ were obtained. Diffraction data was obtained at up to 1.0 Å. The crystal was placed in a cold nitrogen gas stream. The diffraction images of recombinant thaumatin were collected using an ADSQ210 area detector (Rigaku, Tokyo, Japan) at the BL-44XU station of SPring-8 (Hyogo, Japan). The initial data set was collected with a

wavelength of 0.9 Å and the crystal was exposed for 1.0 s to 0.7° oscillations with a 0.7-mm aluminium attenuator for the high resolution data set, and for 1.0 s to 0.7° oscillations with a 1.3-mm aluminium attenuator for the low resolution data set. The data obtained were integrated with the HKL2000 program package [23] from 50 to 1.5 Å and 1.5 to 1.0 Å for the low and high resolution data set, respectively. The integrated intensities were scaled and merged into one dataset. Data collection and structure solution statistics of the recombinant thaumatin I are shown in Supplementary Table 1.

The diffraction images of the native plant thaumatin I were collected using an ADSQ210 area detector (Rigaku, Tokyo, Japan) at the BL-38B1 station of SPring-8 (Hyogo, Japan). The data was collected with a wavelength of 1.0 Å and the crystal was exposed for 1.0 s to 0.7° oscillations. The data obtained were integrated with the HKL2000 program package as described above from 50 to 1.4 Å. Data collection and structure solution statistics are shown in supplementary Table 1.

2.4. Structural refinement and validation

First, the structure of plant thaumatin was determined by molecular replacement using the program MOLREP in the ccp4i suite [24] with the previously reported thaumatin structure (resolution of 1.75 Å) as a reference (PDB code 1thv, [10]). The model-building and refinement were performed using the Coot program [25] and Refmac5, respectively. The $|Fo|-|Fc|$ and $2|Fo|-|Fc|$ maps were used to locate the correct model. Several rounds of refinement were carried out to improve the model by increasing the resolution to 1.39 Å. Water molecules were incorporated where the difference density exhibited values of more than 3.0σ above the mean and the $2|Fo|-|Fc|$ map showed a density of more than 1.0σ. The structure of plant thaumatin at pH 8.0 was refined to a final *R* factor of 14.90%. The coordinate and intensity of plant thaumatin at pH 8.0

have been deposited in the PDB (accession code 3vhf).

The structure of the recombinant thaumatin was determined using the refined plant thaumatin structure mentioned above (3vhf) as a model through rigid-body refinement with the SHELXL97 program [26]. All reflections were included with no σ cutoff; 5% of the data were randomly selected and omitted during refinement for cross validation by means of the free *R*-factor [27]. Refinement of the model with an isotropic *B*-factor against the data up to a resolution of 1.0 Å by SHELXL resulted in an R_{work} of 16.31% and an R_{free} of 18.90%. Subsequent anisotropic *B*-factor refinement against the data to 1.0 Å lowered the R_{work} and R_{free} to 12.08% and 15.63%, respectively (corresponding to a fall in R_{free} of 3.27%). Next, hydrogen atoms were modelled based on the HFIX, and the R_{work} and R_{free} fell to 11.09% and of 14.15%, respectively. To finalize the refinement, the model including H-atoms was refined against all data for 40 cycles using conjugate-gradient least squares minimization, leading to an *R*1 of 11.15% for 106,823 reflections and 10.37% for 94,886 reflections with $Fo > 4\sigma(Fo)$ in the range 10-1.0 Å. The quality of the structure was assessed by using PROCHECK [28] and WHAT IF [29]. The electron density maps and structural images were generated using PyMOL [30]. The coordinate and observed intensity of the recombinant thaumatin I at pH 8.0 have been deposited in the PDBj (accession code 3vjq).

3. Results and discussion

3-1. Overall structure of recombinant thaumatin I

To date 35 structures of thaumatin have been deposited in the Protein Data Bank and four crystal forms (tetragonal, orthorhombic, monoclinic and hexagonal) of thaumatin are known [9,10,13]. Furthermore, there are two types of orthorhombic crystals, that is, orthorhombic (1) (cell dimensions are approximately *a*=51 Å, *b*=54 Å, *c*=70 Å) and orthorhombic (2) (cell dimensions are

approximately *a*=44 Å, *b*= 64 Å, *c*=72 Å). In the present study we investigated a crystal form of orthorhombic (2), whose cell dimensions are *a*=43.636 Å, *b*=63.528 Å and *c*=71.771 Å (Table 1). The final model of the recombinant thaumatin I consists of 207 residues with a total of 1688 protein atoms, 2 glycerol molecules, and 453 water molecules (Figure 1). A single thaumatin molecule is contained in an asymmetric unit. The *R* factor for the final structure is 11.15% for all data, suggesting that the final refined model is of high quality. A Ramachandran plot calculated for the final model showed that 90.5% of the residues are in most favoured regions, 8.9% are in additional allowed regions, and 0.6% are in generously allowed regions. No residues are in disallowed regions (Table 1). The residue located in the generously allowed region is Asp25 which was generally observed in other thaumatin molecules [7,16]. The average *B* factor for main chain, side chain and all atoms was 9.37 $Å^2$, 14.83 $Å^2$, and 15.97 $Å^2$, respectively. The Matthews coefficient *V*m [31], and the solvent content were calculated to be 2.24 $Å^3$/Da and 45.12%, respectively (Table 1). Compared to the tetragonal form of thaumatin I, both the Matthews coefficient and the solvent content are significantly lower, that is, 2.80 $Å^3$/Da and 56.13%, respectively.

3-2. Multiple conformations of side chains of thaumatin at pH 8.0

The electron density map of the recombinant thaumatin I at pH 8.0 allowed the side chains of 13 residues (Glu4, Val13, Arg29, Asn46, Lys49, Asp55, Ser63, Ile65, Arg79, Arg82, Met112, Arg122, and Gln153) to be modelled in two conformations and 1 residue (Ser36) to be modelled in three conformations. Although it seems that the alternative conformations of side chains in plant thaumatin (PDB code 1thv) might not be assigned at a resolution of 1.75 Å [10], in the present study, we could assign 14 alternative side chains in the recombinant thaumatin I at a resolution of 1.0 Å. Recently, Asherie et al. also assigned 11 residues (Arg8, Ser10, Ser36, Glu42, Asp55, Ser63, Lys67, Gln153, Lys174, Pro178 and Ser197) as alternative side chains conformations of plant

thaumatin I (PDB code 2vu7, 1.08 Å, [6]). Since they performed the crystallization in a 10 mM sodium phosphate buffer pH 7.3 containing 250 mM sodium *meso*-tartrate and 2.5% glycerol, *meso*-tartrate might have been affected by the crystal packing around Arg82 and Arg171. Since Arg29 is located near the *meso*-tartrate molecules contact site, it seems that alternative side chain conformations of Arg29 could be assigned in this study because we performed crystallization under conditions without tartrate molecules (Figure 2). Alternative conformations at Arg29 of plant thaumatin I at a resolution of 1.40 Å (3vhf) were also observed under the same crystallization conditions, suggesting the side chain of Arg29 to be flexible in the absence of tartrate molecules.

3-3. Comparison of r.m.s. deviation and temperature factor values

The differences in r.m.s. deviation for Cα atoms between the final refined structure of the orthorhombic form of the recombinant thaumatin at pH 8.0 (PDB code 3vjq) and those of plant thaumatin I at pH 7.3 (PDB code 2vu7, $P2_12_12_1$) were investigated (Figure 3). The most significance difference in r.m.s.d. values was observed in the large disulfide-rich region of domain II, especially residues 154-164, suggesting a loop region in domain II of thaumatin to be affected by the change in pH from 7.3 to 8.0 (closed circles). Next we attempted to compare the orthorhombic structure (PDB code 3vjq) to the tetragonal form of the recombinant thaumatin I (PDB code 3al7, $P4_12_12$) prepared at pH 6.5 [7]. The results showed that residues 154-164 had high r.m.s.d. values like the orthorhombic crystal, suggesting a loop region in domain II of thaumatin to be affected by pH change. Besides these regions, C-terminal residues had high r.m.s.d. values (closed triangles).

Clear changes in r.m.s.d values for a change from pH 7.3 to 8.0 or 6.5 to 8.0 are detectable in a loop region in domain II of thaumatin. Next we attempted to compare a high resolution tetragonal structure of the recombinant thaumatin I (PDB code 3al7) at pH 6.5 against 2vhk (pH 7.3). No

significant difference in r.m.s.d values was observed in the loop region in domain II on the change from pH 6.5 to 7.3, suggesting the substantial change in the loop region in domain II to be specific to the change to pH 8.0 (Figure 3, closed square).

Since the thermal factor is closely related to an atom's mean square amplitude of vibration, it is worth comparing high resolution structures at different pH. At pH 8.0, residues with more than 2.5-fold the average thermal factor, *B*, for main chains included Gly141 (24.9 $Å^2$), Thr160 (24.0 $Å^2$), Thr161 (29.1 $Å^2$), Gly162 (41.1 $Å^2$) and Lys163 (43.5 $Å^2$). Residues with more than 2.5-fold the average for side chains were Lys137 (52.4 $Å^2$) and Lys163 (57.3 $Å^2$). In contrast, at pH 7.3, Thr160 (24.2 $Å^2$), Thr161 (28.3 $Å^2$), Gly162 (29.5 $Å^2$) and Lys163 (26.0 $Å^2$) had more than 2.5-fold the average for main chains and no residues had more than a 2.5-fold higher value for side chains. These results suggested the increase in *B*-factor values for Lys137, Lys163 and Lys187 to be induced by pH change.

Thus, a comparison of high resolution structures at different pH values, 3vjq (resolution of 1.0 Å, pH 8.0) and 2vu7 (resolution of 1.08 Å, pH 7.3), would reveal the subtle conformational change induced by a change in pH. It was suggested that lysine residues were involved in the heat-inactivation of thaumatin and a free sulfhydryl residue produced via the β-elimination of disulfide bond by heating at a pH above 7 [20]. Although thaumatin contains 11 lysine residues, only Lys137, Lys163, and Lys187 have high temperature factors under alkaline conditions. These results suggested an increase in the mobility of lysine residues as well as the large disulfide-rich region in domain II under alkaline conditions to play an important role in the heat aggregation of thaumatin at a pH above 7.

The structural requirements necessary for the sweetness of thaumatin molecules have been investigated using chemical modifications and site-directed mutagenesis, suggesting the lysine residues located on the cleft-containing side to play an important role [21, 32-34]. K137, K163 and

K187 are also located on the cleft-containing side, and the basicity of these lysine residues is important to the sweetness of thaumatin as well. In the present study, we determined the atomic structure of thaumatin at pH 8.0. Understanding the precise structural features of thaumatin under alkaline conditions should provide new insights into the denaturation of thaumatin by heat treatment. These findings appear to offer a structural basis for use in food products and the design of thermo stable proteins.

Acknowledgments

This work was supported by Grants-in-aid for Young Scientists (B) (T.M., no.19780074) and Scientific Research (C) (T.M., no. 22580105) from The Japan Society for the Promotion of Science. The synchrotron radiation experiments were performed at BL38B1 and BL44XU in SPring-8 with the approval of the Japan Synchrotron Radiation Research Institute (JASRI) (proposal number 2009A1096, 2009B1379, 2010A6538, 2010B1064).

References

[1] H. van der Wel, K. Loeve, Isolation and characterization of thaumatin I and II, the sweet-tasting proteins from Thaumatococcus daniellii Benth, Eur. J. Biochem. 31 (1972) 221-225.

[2] P.A. Temussi, Why are sweet proteins sweet? Interaction of brazzein, monellin and thaumatin with the T1R2-T1R3 receptor, FEBS Lett. 526 (2002) 1-4.

[3] P.A. Temussi, Natural sweet macromoleculars: how sweet protein work, Cell Mol. Life Sci. 63 (2006) 1876-1888.

[4] T. Masuda, N. Kitabatake, Developments in biotechnological production of sweet proteins, J.

Biosci. Bioeng. 102 (2006) 375-389.

[5] K. Etheridge, The sales and marketing of talin, in: M. Witty, J.D. Higginbotham (Eds.), Thaumatin, CRC Press, Boca Raton Florida, 1994, pp. 47-59.

[6] N. Asherie, J. Jakoncic, C. Ginsberg, A. Greenbaum, V. Stojanoff, B.J. Hrnjez, S. Blass, J. Berger, Tartrate chirality determines thaumatin crystal habit, Cryst. Growth Des. 9 (2009) 4189–4198.

[7] T. Masuda, K. Ohta, B. Mikami, N. Kitabatake, High-resolution structure of the recombinant sweet-tasting protein thaumatin I, Acta Crystallogr. Sect. F67 (2011) 652-658.

[8] H. van der Wel, T.C. van Soest, E.C. Royers, Crystallization and crystal data of thaumatin I, a sweet-tasting protein from Thaumatococcus daniellii benth, FEBS Lett. 56, (1975) 316-317.

[9] C.M. Ogata, P.F. Gordon, A.M. de Vos, S.H. Kim, Crystal structure of a sweet tasting protein thaumatin I, at 1.65 Å resolution, J. Mol. Biol. 228, (1992) 893-908.

[10] T-P. Ko, J. Day, A. Greenwood, A. McPherson, Structures of three crystal forms of the sweet protein thaumatin, Acta Crystllogr. Sect. D50 (1994) 813-825.

[11] C. Sauter, B. Lorber, R. Giegé, Towards atomic resolution with crystals grown in gel: the case of thaumatin seen at room temperature, Proteins. 48 (2002) 146-150.

[12] C. Charron, A. Kadri, M.-C. Robert, R. Giegé, B. Lorber, Crystallization in the presence of glycerol displaces water molecules in the structure of thaumatin. Acta Crystllogr. Sect. D58 (2002) 2060-2065.

[13] C. Charron, R. Giegé, B. Lorber, Structure of thaumatin in a hexagonal space group: comparison of packing contacts in four crystal lattices, Acta Crystllogr. Sect. D60 (2004) 83-89.

[14] S.C. Teixeira, M.P. Blakeley, R.M. Leal, E.P. Mitchell, V.T. Forsyth, A preliminary neutron

crystallographic study of thaumatin, Acta Crystllogr. Sect. F64 (2008) 378-381.

[15] S.C. Teixeira, M.P. Blakeley, R.M. Leal, S.M. Gillespie, E.P. Mitchell, V.T. Forsyth, Sweet neutron crystallography, Acta Crystllogr. Sect. D66 (2010) 1139-1143.

[16] T. Masuda, K. Ohta, F. Tani, N. Kitabatake, Crystal structure of the sweet-tasting protein thaumatin II at 1.27 Å, Biochem. Biophys. Res. Commun. 410 (2011) 457-460.

[17] N. Ide, T. Masuda, N. Kitabatake, Effects of pre- and pro-sequence of thaumatin on the secretion by Pichia pastoris, Biochem. Biophys. Res. Commun. 363 (2007) 708–714.

[18] T. Masuda, N. Ide, K. Ohta, N. Kitabatake, High-yield secretion of the recombinant sweet-tasting protein thaumatin I, Food Sci. Technol. Res. 16 (2010) 585-592.

[19] H. van der Wel, R.B. Iyengar, J. van Brouwershaven, P.D. van Wassenaar, W.J. Bel, F.J. van der Ouderaa, Assignment of the disulphide bonds in the sweet-tasting protein thaumatin I, Eur. J. Biochem. 144 (1984) 41-45.

[20] R. Kaneko, N. Kitabatake, Heat-induced formation of intermolecular disulfide linkages between thaumatin molecules that do not contain cysteine residues, J. Agric. Food Chem. 47 (1999) 4950-4955.

[21] R. Kaneko, N. Kitabatake, Sweetness of sweet protein thaumatin is more thermoresistant under acid conditions than under neutral or alkaline conditions, Biosci. Biotechnol. Biochem. 65 (2001) 409-413.

[22] T. Masuda, Y. Ueno, N. Kitabatake, High yield secretion of the sweet-tasting protein lysozyme from the yeast Pichia pastoris, Protein Expr. Purif. 39 (2005) 35-42.

[23] Z. Otwinowski, W. Minor, Processing of X-ray crystallographic data collected in oscillation mode, Methods Enzymol. 276 (1997) 307–326.

[24] A. Vagin, A. Teplyakov, MOLREP: an Automated Program for Molecular Replacement, J. Appl. Cryst. 30 (1997) 1022–1025.

[25] P. Emsley, K. Cowtan, Coot: model-building tools for molecular graphics, Acta Crystllog. Sect. D60 (2004) 2126–2132.

[26] M. Sheldrick, T.R. Schneider, SHELXL: high-resolution refinement, Methods Enzymol. 277 (1997) 319–343.

[27] A.T. Brünger, Free R value: a novel statistical quantity for assessing the accuracy of crystal structures. Nature, 355, (1992) 472–475.

[28] R.A. Laskowski, M.W. MacArthur, D.S. Moss, J. M. Thornton, PROCHECK: a program to check the stereochemical quality of protein structures, J. Appl. Cryst. 26 (1993) 283-291.

[29] M.L. Hekkelman, T.A. Te Beek, S.R. Pettifer, D. Thorne, T.K. Attwood, G. Vriend, WIWS: a protein structure bioinformatics Web service collection, Nucleic Acids Res. 38 (2010) W719-723.

[30] W.L. DeLano, (2002). The PyMOL Molecular Graphics System. DeLano Scientific, San Carlos, CA, USA. 2002.

[31] B.W. Matthews, Solvent content of protein crystals, J. Mol. Biol. 33 (1968) 491-497.

[32] S.H. Kim, J.L. Weickmann, Crystal structure of thaumatin I and its correlation to biochemical and mutational studies. in: M. Witty, J.D. Higginbotham (Eds.), Thaumatin, CRC Press, Boca Raton Florida, 1994, pp. 135-149.

[33] K. Ohta, T. Masuda, N. Ide, N. Kitabatake, Critical molecular regions for elicitation of the sweetness of the sweet-tasting protein, thaumatin I, FEBS J. 275 (2008) 3644–3652.

[34] K. Ohta, T. Masuda, F. Tani, N. Kitabatake, The cysteine-rich domain of human T1R3 is necessary for the interaction between human T1R2-T1R3 sweet receptors and a sweet-tasting

protein, thaumatin, Biochem. Biophys. Res. Commun. 406 (2011) 435–438.

Legends to Figures

Figure 1

Overall structure of the recombinant thaumatin I. (A) Two residues, Lys67 and Arg82, critical for sweetness are shown in blue. The residues from 154 to 164 in the large disulfide-rich region of domain II are indicated in red. The average *B*-factors over side chains in Lys137 (52.4 $Å^2$), Lys163 (57.3 $Å^2$) and Lys187 (42.9 $Å^2$) are shown in yellow. Two glycerol molecules are indicated in green. (B) The spectrum of the average *B*-factors is indicated from minimum (blue = 0) to maximum (red = 30).

Figure 2

The model and electron density of the recombinant thaumatin around Arg29. The σA-weighted 2mFo-DFc maps contoured at 1.0σ are shown in blue and mFo-DFc maps omitting hydrogen atoms contoured at 3.0σ and -3.0σ are shown in green and red, respectively.

Figure 3

The superposition of the coordinates of Cα atoms of thaumatin at different pH.

Histograms of r.m.s.d. values of Cα atoms with the residue number. The structure of the orthorhombic form of the recombinant thaumatin at pH 8.0 (PDB code 3vjq) and of plant thaumatin I at pH 7.3 (PDB code 2vu7, $P2_12_12_1$) were analyzed (closed circles). The orthorhombic form (PDB code 3vjq) against the tetragonal structure of the recombinant thaumatin I (PDB code 3al7, $P4_12_12$) prepared at pH 6.5 was investigated (closed triangles). The tetragonal structure of the recombinant

thaumatin I (PDB code 3al7) at pH 6.5 against 2vhk (pH 7.3) was examined (closed square).

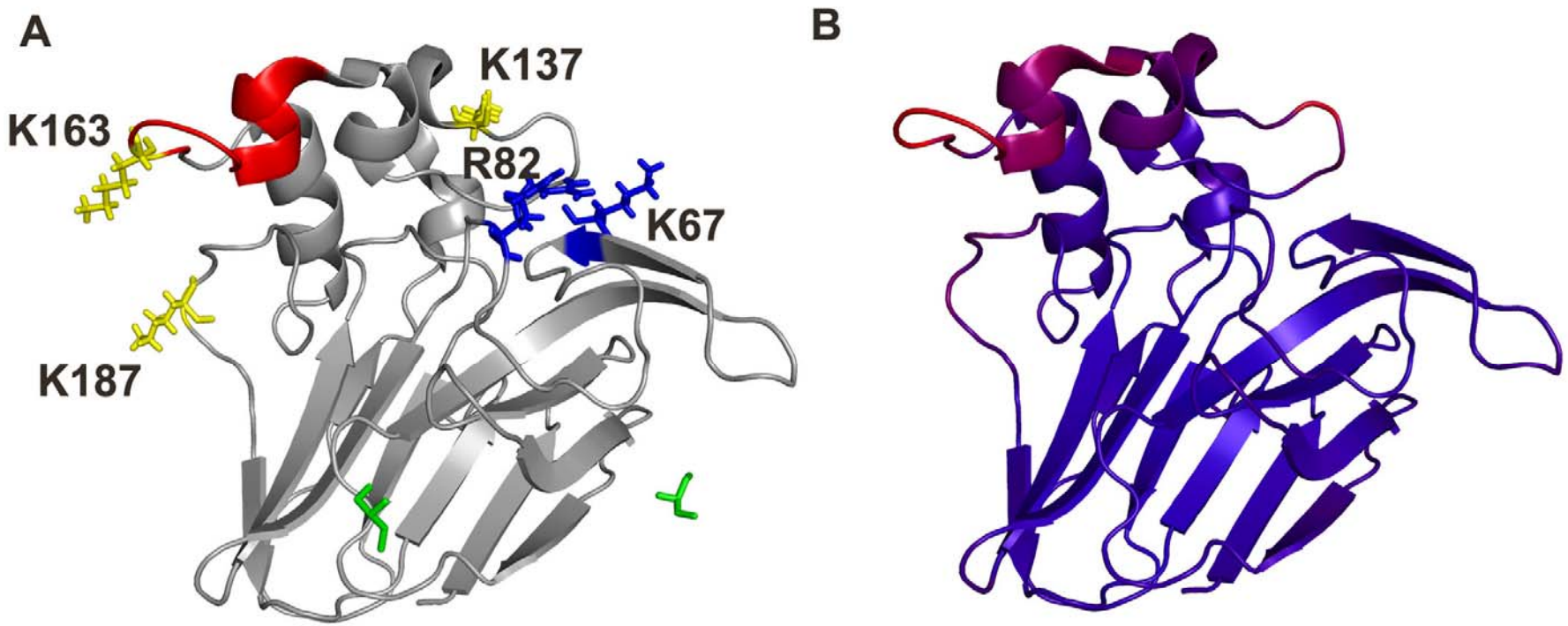

Figure 1

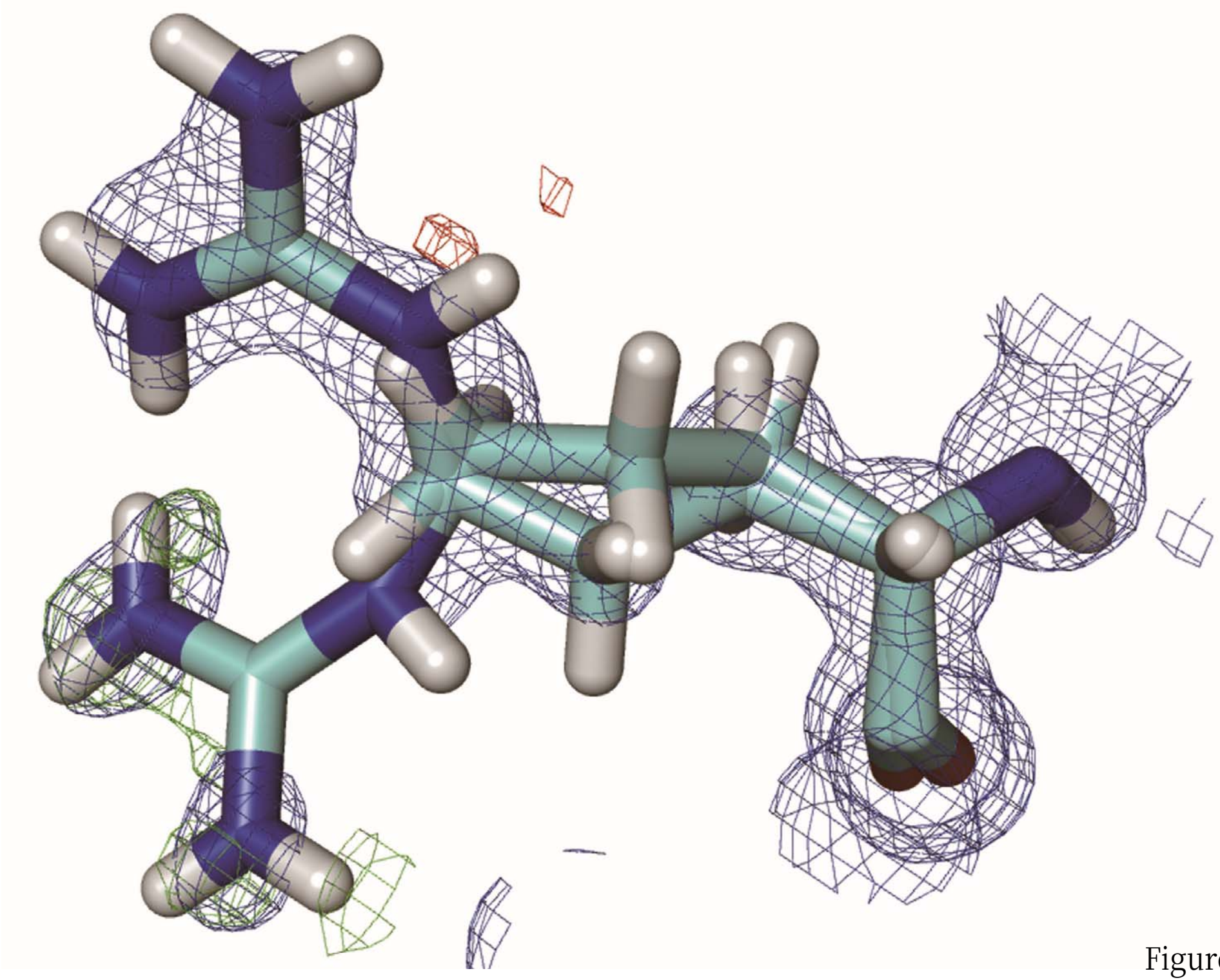

Figure 2

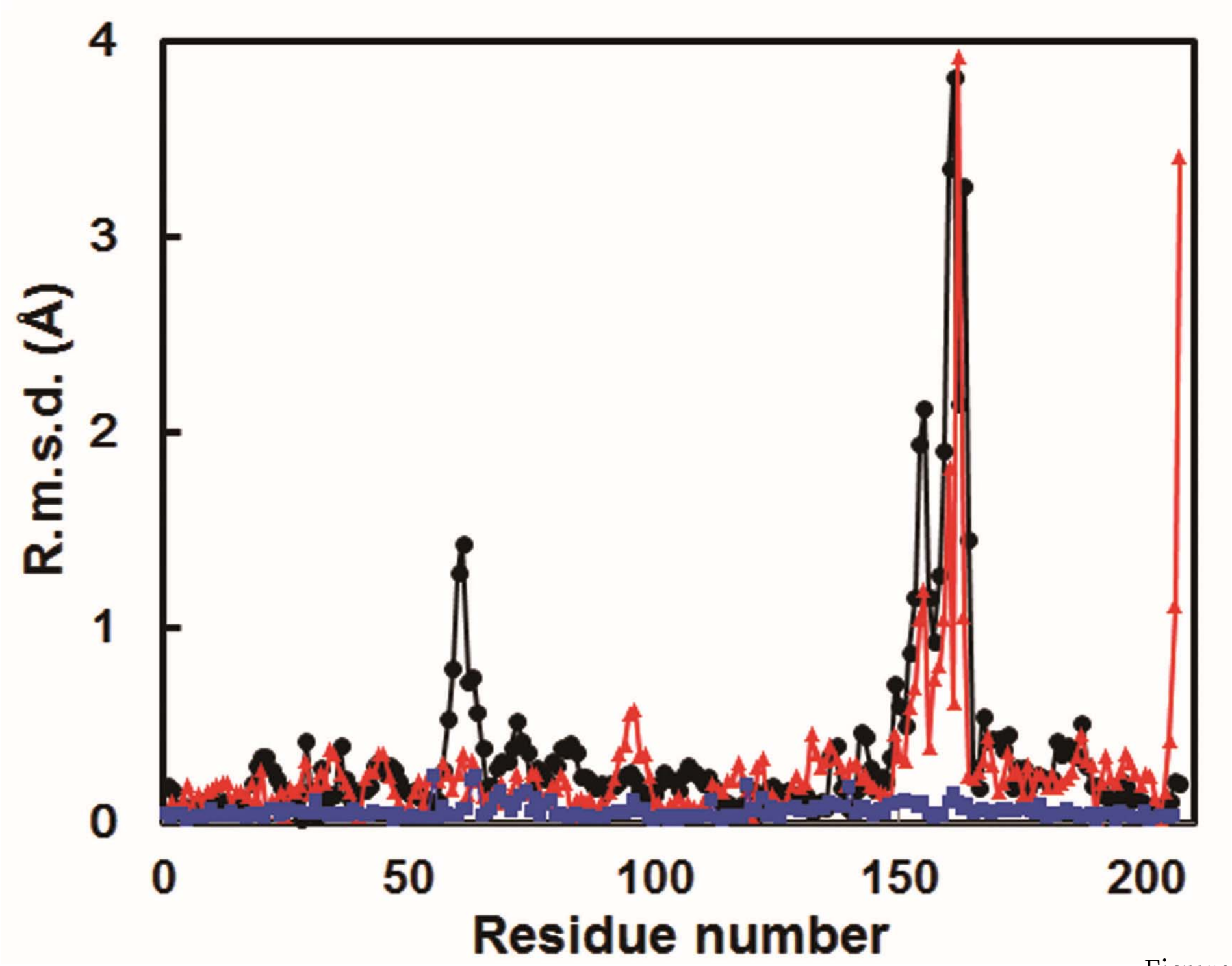

Figure 3